Ku80 Deletion Suppresses Spontaneous Tumors and Induces a p53-Mediated DNA Damage Response

Valerie B. Holcomb,[1] Francis Rodier,[2,3] YongJun Choi,[1] Rita A. Busuttil,[3] Hannes Vogel,[4] Jan Vijg,[5] Judith Campisi,[2,3] and Paul Hasty[1]

[1]Department of Molecular Medicine, Institute of Biotechnology, The University of Texas Health Science Center at San Antonio, San Antonio, Texas; [2]Life Sciences Division, Lawrence Berkeley National Laboratory, Berkeley, California; [3]Buck Institute for Age Research, Novato, California; [4]Department of Pathology, Stanford University Medical Center, Palo Alto, California; and [5]Albert Einstein College of Medicine, Bronx, New York

Abstract

Ku80 facilitates DNA repair and therefore should suppress cancer. However, *ku80*$^{-/-}$ mice exhibit reduced cancer, although they age prematurely and have a shortened life span. We tested the hypothesis that Ku80 deletion suppresses cancer by enhancing cellular tumor-suppressive responses to inefficiently repaired DNA damage. In support of this hypothesis, Ku80 deletion ameliorated tumor burden in *APC*^{MIN} mice and increased a p53-mediated DNA damage response, DNA lesions, and chromosomal rearrangements. Thus, contrary to its assumed role as a caretaker tumor suppressor, Ku80 facilitates tumor growth most likely by dampening baseline cellular DNA damage responses. [Cancer Res 2008;68(22):9497–502]

Introduction

DNA damage drives malignant tumorigenesis and processes that ameliorate this damage, and its sequelae can be categorized as either gatekeeper or caretaker tumor suppressors, depending on their mode of action (1). Gatekeepers control checkpoints that determine the fate of damaged cells, whereas caretakers prevent DNA damage or facilitate its repair (2). DNA damage checkpoint machineries monitor the genome for problems that adversely affect DNA replication or mitosis and halt cell cycle progression to allow time for repair. If the damage is severe or irreparable, these machineries engage either cell death (apoptosis) or permanent cell cycle arrest (cellular senescence) pathways. These cellular damage responses are crucial anticancer mechanisms and require the activity of potent tumor suppressor proteins, such as p53, which are frequently mutated in both heritable and spontaneous cancers (3). Caretakers are also considered to be tumor suppressors because genomic instability drives cancer progression (4) and some heritable forms of cancer are due to mutations in DNA repair genes (5). Unlike gatekeepers, defects in caretakers are not commonly seen in spontaneous tumors. Thus, gatekeepers seem to be more important than caretakers for suppressing spontaneous tumors.

Nonhomologous end joining (NHEJ) repairs DNA double-strand breaks by joining ends without using a homologous template strand and has been described as a caretaker (6, 7). Known components of mammalian NHEJ include Ku70, Ku80, DNA-dependent protein kinase catalytic subunit (DNA-PK$_{CS}$), Artemis, Xrcc4, DNA ligase IV, and Xrcc4-like factor. Ku70 and Ku80 form a heterodimer (termed Ku) that complexes with the 460-kDa DNA-PK$_{CS}$ to form a holoenzyme referred to as DNA-dependent protein kinase (DNA-PK). Artemis and DNA-PK$_{CS}$ form a complex that opens hairpins and processes overhangs. These DNA ends are then ligated by Xrcc4-DNA ligase IV in a complex with Xrcc4-like factor. By rapidly processing and ligating broken DNA, NHEJ suppresses general genomic instability.

Ku80 deletion causes an increase in the incidence of DNA double-strand breaks (8) and chromosomal aberrations (9) and also increases the incidence of cancer in mice that carry mutations in additional genes like *p53* (10, 11). Based on these observations, Ku80 has been termed a tumor suppressor in the caretaker category (6, 7). However, this interpretation should be viewed with caution because p53-defective mice are rare or nonexistent in nature; thus, Ku80 may not have been selected for a caretaker function. Interestingly, *ku80*$^{-/-}$ mice have a reduced, rather than an increased, cancer incidence, although they age prematurely and have a shortened life span (9, 12, 13). We proposed that the low cancer incidence in *ku80*$^{-/-}$ mice is due to the Ku80 deletion and is not an indirect consequence of the shortened life span. We further hypothesized that *ku80*$^{-/-}$ cells exhibit persistent gatekeeper responses, owing to inefficiently repaired DNA breaks, and that these responses ultimately impede oncogenesis.

To test this hypothesis, we analyzed *ku80*$^{-/-}$ mice in cancer-prone backgrounds that have either defective or intact gatekeeper responses, predicting that Ku80 deletion will exacerbate oncogenesis in gatekeeper-defective mice but ameliorate oncogenesis in gatekeeper-intact mice. In support of this idea, we previously showed that Ku80 deletion enhances p53-dependent cellular senescence in cultured fibroblasts (10) and exacerbates the development of pro-B cell lymphomas (10) and medulloblastomas (11) in p53-deficient mice. Thus, p53 affects the Ku80-mutant phenotype to enhance cellular senescence and suppress at least two forms of cancer. However, neither pro-B cell lymphomas nor medulloblastomas are common spontaneous tumors in mice, leaving open the question of whether gatekeeper responses are indeed responsible for the low levels of spontaneous cancer in *ku80*$^{-/-}$ mice.

Here, we evaluate the effect of Ku80 deletion on spontaneous oncogenesis and investigate the possibility that Ku80 deficiency induces p53-mediated DNA damage responses to poorly repaired DNA lesions. To study spontaneous oncogenesis, we analyzed *APC*^{MIN} mice deleted for Ku80 because they develop spontaneous intestinal tumors at high incidence within the life span of *ku80*$^{-/-}$ mice. Importantly, *APC*^{MIN} mice retain functional DNA damage

Note: Current address for V.B. Holcomb: Division of Nutritional Sciences, Department of Human Ecology, The University of Texas at Austin, 1 University Station, Austin, TX 78712.

Requests for reprints: Paul Hasty, The University of Texas Health Science Center at San Antonio, 15355 Lambda Drive, San Antonio, TX 78245-3207. Phone: 210-567-7278; Fax: 210-567-7247; E-mail: hastye@uthscsa.edu.

doi:10.1158/0008-5472.CAN-08-2085

checkpoints (14). We show that Ku80 deletion significantly reduces tumor burden in APC^{MIN} mice. In both murine embryonic fibroblasts (MEF) and small intestine, we show that Ku80 deletion induces a p53-mediated DNA damage response that elevates p21 expression, causes persistent DNA damage, and increases chromosomal rearrangements. These findings indicate that Ku80 deletion reduces spontaneous oncogenesis, most likely by inducing a p53-mediated DNA damage response to persistent DNA lesions.

Materials and Methods

Phenotypic observations/mouse husbandry. We crossed $Ku80^{+/-}$ mice (C57BL/6J × 129SvEv cross; ref. 15) to APC^{MIN} mice (The Jackson Laboratory; C57BL/6J-*ApcMin*/J) to generate all genotypes presented in Fig. 1. Thus, all mice are controlled for genetic background and environment because they are brothers, sisters, and cousins raised under identical conditions (the same room, cages, bedding, and food). Mice were housed in a specific pathogen-free environment in microisolator cages and observed five to six times per week for their entire life spans. Moribund mice (significant loss of weight and responsiveness) were monitored multiple times per day and euthanized when incapable of reaching the water source. Morbidities were scored by Kaplan-Meier analysis and statistical significance was determined by the log-rank test. Euthanized mice were examined by necropsy and organs were removed and fixed for histology. Genotyping has been described for *Ku80* (9) and APC^{MIN}.[6]

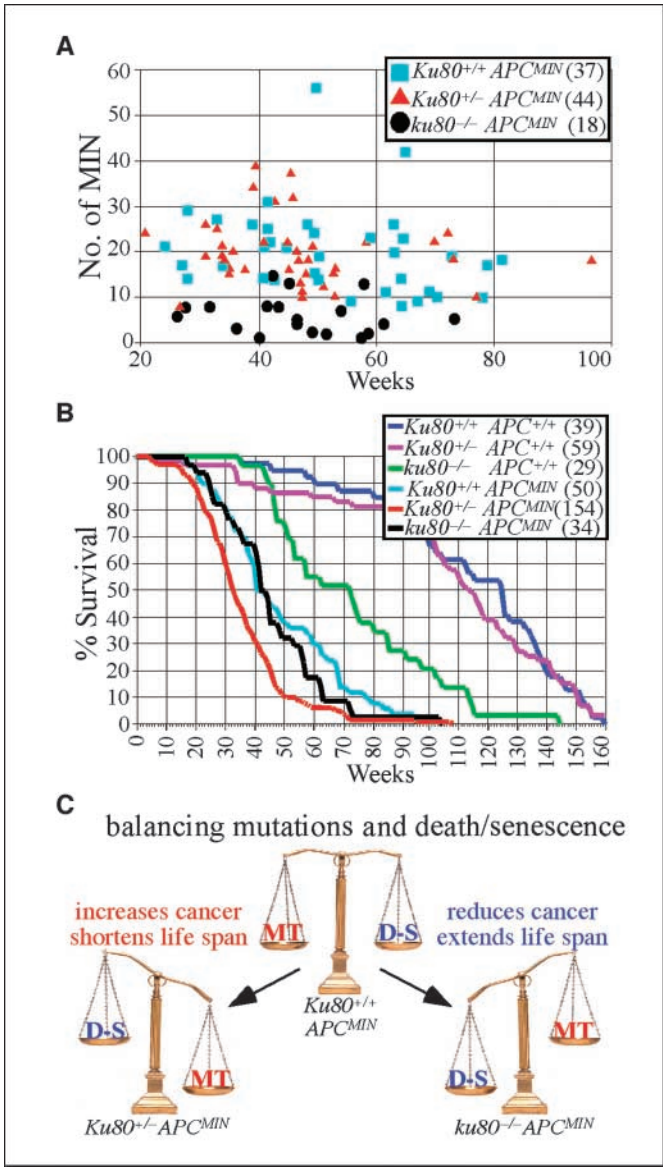

Figure 1. Ku80 deletion reduces intestinal tumors in APC^{MIN} mice. *A,* number of MIN tumors for APC^{MIN} mice with +/+, +/−, and −/− Ku80 genotypes. Number of mice observed indicated in parentheses. *B,* life spans for all cohorts of mice. Number of mice observed indicated in parentheses. *C,* balance between DNA mutations (*MT*) that exacerbate cancer and cell death or senescence (*D-S*) that ameliorate cancer.

For mutation analysis, $Ku80^{+/-}$ mice on a C57/BL/6J background were crossed with C57BL/6J pUR288-(lacZ)-transgenic mice line 60 (integration sites on chromosomes 3 and 4) and bred to generate $ku80^{-/-}$ animals hemizygous for pUR288-*lacZ*. $Ku80^{+/+}$ littermate animals served as wild-type controls. The animals were maintained in the animal facilities of the University of Texas Health Science Center at San Antonio on a 12-h light/12-h dark cycle at a standard temperature of 23°C. Standard lab chow (Harlan Teklad) and water were supplied *ad libitum*. Animals were sacrificed by CO_2 inhalation followed by cervical dislocation at 4 to 5 mo of age.

MEF isolation. To generate MEFs, 13.5-d-old embryos were separated from the placenta and surrounding membranes, rinsed in 70% ethanol, and placed into 1.5-mL Eppendorf tubes containing PBS. Repeated pipetting with a transfer pipette finely minced the embryos. Trypsin-EDTA was added to the tubes, which were incubated at 37°C for 15 min; the contents were seeded onto 15-cm plates in M10 medium (MEM with 10% fetal bovine serum, 2 mmol/L glutamine, 30 mg penicillin/mL, 50 mg streptomycin/mL). This culture was considered passage 0. All cultures were maintained in a 3% O_2 and 5% CO_2 atmosphere.

Protein extraction and Western blot. Whole-cell lysates were prepared from MEFs or mouse small intestine. Tissues were collected, washed with PBS, and snap-frozen in liquid N2. Frozen tissues were ground into a powder using a mortar and pestle and suspended in 150 mmol/L NaCl, 10 mmol/L Tris-HCl (pH 8.0), 1 mmol/L EDTA (pH 8.0), 1% NP40, and 1% sodium deoxycholate containing protease inhibitors (Complete, Mini protease inhibitor tablets; Roche; lysis buffer). After extensive homogenization and sonication, extracts were clarified by centrifugation (10 min at 10,000 × *g*). MEFs were grown to confluency on 15-cm plates, washed with PBS, trypsinized, collected by centrifugation, and lysed in lysis buffer. Extracts were clarified by centrifugation for 10 min at 10,000 × *g*. Cell or tissue extracts (80 μg) were resolved by 10% SDS-PAGE and proteins were detected by Western blot with mouse monoclonal antibodies to p53 (Ab-1, clone PAb 240, LabVision), phospho-p53 (Ser^{15}; Cell Signaling Technology), p21 (Santa Cruz Biotechnology), p16 (sc-1207, Santa Cruz Biotechnology), or β-actin (Abcam) according to the manufacturer's instructions.

Irradiation. Mice were treated with a single dose of whole-body ^{137}Cs γ-irradiation (Mark1 γ-radiation source, Shepard and Associates) of 8 Gy at an exposure rate of 2.44 Gy/min and sacrificed 4 h later to collect tissues. MEFs for Fig. 2 were treated with a single dose of 5 Gy at an exposure rate of 2.44 Gy/min and lysed in lysis buffer 2 h later. Control mice and MEFs were placed in the radiation chamber for the same amount of time but were not irradiated. MEFs for Fig. 4 were cultured on glass slides and treated with a single dose of 10-Gy X-ray irradiation at rates ≥0.75 Gy/min using a Pantak X-ray generator (320 kV/10 mA with 0.5-mm copper filtration) and lysed in lysis buffer 2 h later.

RNA extraction and cDNA synthesis. Total RNA was prepared by grinding frozen small intestine into a powder using a mortar and pestle. The powdered tissue was homogenized in Trizol reagent (Invitrogen) according to the manufacturer's instructions and reverse transcribed using oligo dT (SuperscriptII, Invitrogen).

Real-time reverse transcription-PCR. Primers used for quantitative reverse transcription-PCR (RT-PCR) were as follows: p21, forward

[6] http://jaxmice.jax.org/strain/002020.html

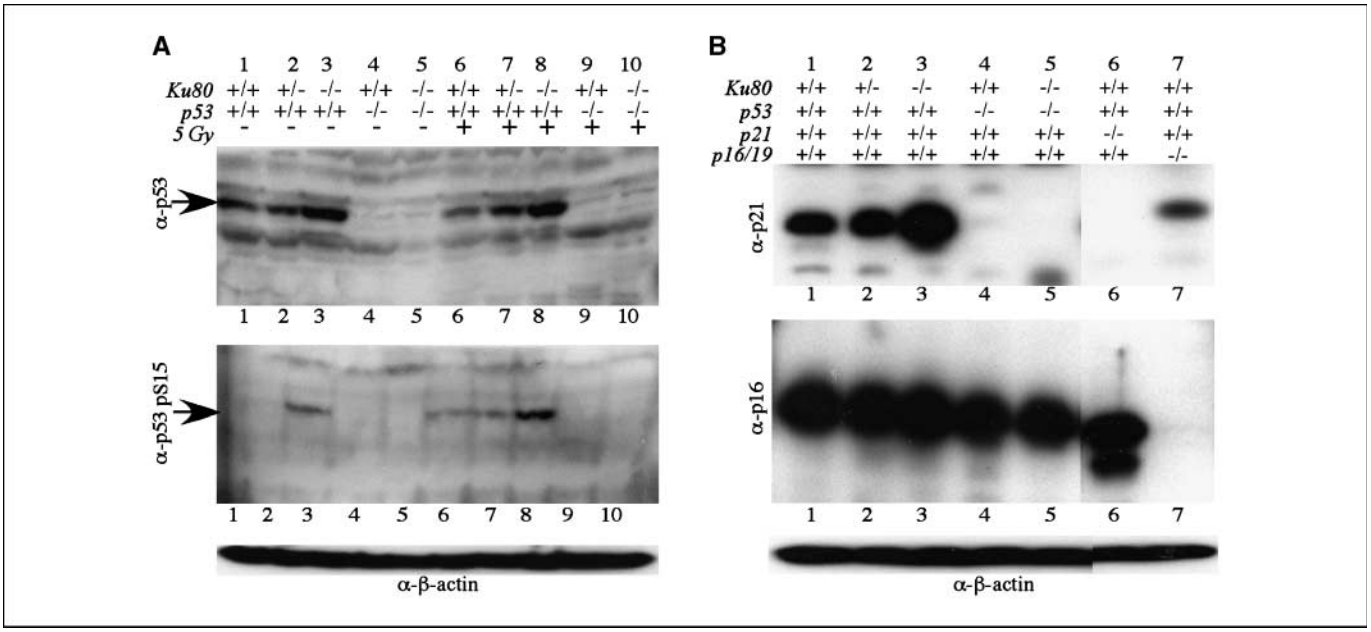

Figure 2. Ku80 deletion increases p53-mediated DNA damage response in MEFs. *A* and *B,* Western blots of passage 3 MEFs. *A,* total p53 (*top, arrow*), p53 pS15 (*middle, arrow*), and β-actin (*bottom*). *B,* total p21 (*top*), p16 (*middle*), and β-actin (*bottom*).

5′-CCAGGCCAAGATGGTGTCTT-3′ and reverse 5′-TGAGAAAGGATCAGCCATTGC-3′; murine double minute-2 (MDM2), forward 5′-TGTCTGTGTCTACCGAGGGTG-3′ and reverse 5′-TCCAACGGACTTTAACAACTTCA-3′; KILLER/DR5, forward 5′-GAGGGTATTGACTACACCAGCC-3′ and reverse 5′-ATGTTGCATCGGGTTTCTACG-3′; GADD45a, forward 5′ CTCGGCTGCAGAGCAGAAGA-3′ and reverse 5′-GGCACAGTACCACGTTATCG-3; BAX, forward 5′-GACAGGGGCCTTTTTGCTA-3′ and reverse 5′-TGTCCACGTCAGCAATCATC-3′; glyceraldehyde-3-phosphate dehydrogenase (GAPDH), forward 5′-CCTGTTCGACAGTCAGCCG-3′ and reverse 5′-CGACCAAATCCGTTGACTCC-3′. Quantitative RT-PCR was done using an Applied Biosystems 7900HT Fast Real-time PCR System (Applied Biosystems) and Absolute SYBR Green ROX Mix (ABgene). The $\Delta\Delta C_t$ method of relative quantification was used to calculate fold expression; p21 (MDM2, KILLER/DR5, and GADD45a BAX) RNA levels were normalized to GAPDH levels; and all reactions were done in triplicate.

Immunostaining. MEFs were plated at 5×10^4 per well in four-well chamber slides and cultured at 3% O_2 for 5 d, as described (25). Cells were washed with PBS, fixed with 4% paraformaldehyde in PBS for 10 min at room temperature, permeabilized with 0.5% Triton X-100 for 10 min, blocked for 30 min, and incubated overnight at 4°C with primary antibody. After washing thrice with PBS, cells were incubated with secondary antibody for 45 min at room temperature, washed once with PBS, and again with PBS containing 4′,6-diamidino-2-phenylindole (1 μg/mL). The cells were photographed using a Nikon Eclipse 800 microscope with a 40× objective and Nikon Digital Camera DXM1200. The primary antibody for p53 binding protein 1 (53BP1) was a rabbit polyclonal from Bethyl (BL182) and the secondary antibody was a donkey anti-rabbit conjugated to Alexa Fluor 594 from Molecular Probes. The primary antibody for γ-H2AX was a mouse monoclonal from Upstate (anti–γ-H2AX Ser^{139} antibody, clone JBW301) and the secondary antibody was a donkey anti-mouse conjugated to Alexa Fluor 488 from Molecular Probes.

Plasmid rescue and mutation analysis. DNA was isolated by phenol/chloroform extraction, as described (16). Briefly, 20 to 30 μg genomic DNA were digested with *Hin*dIII (Roche) for 1 h in the presence of magnetic beads (Dynal) precoated with lacZ-lacI fusion protein. The beads were washed thrice to remove excess genomic DNA, and plasmids were eluted from the beads with isopropyl-L-thio-B-D-galactopyranoside. After circularization of the plasmids with T4 DNA ligase, they were ethanol precipitated and used to transform *Escherichia coli* C (ΔlacZ, galE$^-$) cells. One thousandth of the transformed cells was plated on a titer plate containing 5-bromo-4-chloro-3-indolyl-β-D-galactopyranoside (X-gal), and the remainder on a selective plate containing phenyl-β-D-galactopyranoside. The plates were incubated for 15 h at 37°C. Mutant frequencies were determined from the number of colonies on the selective plate divided by the number of colonies on the titer plate, times 1,000. Each mutant frequency is based on at least 300,000 recovered plasmids.

Mutant classification and characterization. Mutant colonies from the selective plates were grown at 37°C overnight in 96-well round-bottomed plates containing Luria-Bertani medium, kanamycin, and ampicillin. One microliter was then plated on X-gal to screen for galactose-insensitive host cells and this background was subtracted. One microliter was added to a PCR mix and the DNA amplified as described (16). The PCR products were digested with *Ava*I and size separated on a 1% agarose gel. Mutant plasmids with restriction patterns resembling the wild-type pattern were classed as "no-change" mutations, whereas those deviating from the wild-type restriction pattern were classified as "size-change" mutations. Approximately 48 mutants per condition were analyzed. LacZ genes of selected mutant plasmids were prepared for sequencing by the University of California, Davis sequencing facility. The chromatograms were analyzed with Sequencher (Gene Codes). The primers used for the sequence reactions were described (16).

Results and Discussion

Ku80 deletion ameliorates tumor burden for APC^{MIN} mice. We crossed $Ku80^{+/-}$ (15) and APC^{MIN} (The Jackson Laboratory) mice to determine the effect of Ku80 deletion on oncogenesis. The *APC* gene is mutated in people with familial adenomatous polyposis coli (17, 18). Similar to humans, mice with *APC* mutations are predisposed to multiple intestinal neoplasias (MIN), both adenomas and adenocarcinomas. $APC^{MIN/MIN}$ embryos die from primitive ectoderm failure before gastrulation (19); therefore, cancer can be observed only in heterozygote mice. $APC^{+/MIN}$ (termed APC^{MIN}) mice die from anemia caused by MIN (20, 21). APC down-regulates the Wnt signaling pathway by associating with β-catenin and controls cellular proliferation (22). Importantly, p53 deficiency enhances the multiplicity and invasiveness of intestinal

adenomas in APC^{MIN} mice (14). We therefore reasoned that Ku80 deficiency should suppress the MIN phenotype if it activates p53 responses.

$Ku80^{+/-}$ APC^{MIN} breeding pairs generated cohorts for all genotypes. All APC^{MIN} cohorts, independent of Ku80 status, developed intestinal neoplasias. We counted MIN at the end of life and found that complete Ku80 deficiency ($ku80^{-/-}$) reduced MIN by ~67% (Fig. 1*A*; $P < 0.0001$, nonparametric Wilcoxon rank sum test). On average, $Ku80^{+/+}APC^{MIN}$ and $Ku80^{+/-}APC^{MIN}$ mice developed 20.0 and 18.9 tumors per intestine, whereas $ku80^{-/-}APC^{MIN}$ mice exhibited only 6.2 tumors per intestine. Thus, complete Ku80 deficiency substantially reduced the total number of adenomas and adenocarcinomas at the end of life for APC^{MIN} mice.

We next determined the effect of this significant reduction in cancer incidence on life span. $ku80^{-/-}APC^{MIN}$ mice survived longer than $Ku80^{+/-}APC^{MIN}$ mice (Fig. 1*B*; $P > 0.006$, log-rank test), consistent with Ku80 deficiency suppressing cancer development. However, $Ku80^{+/+}APC^{MIN}$ mice also lived longer than $Ku80^{+/-}APC^{MIN}$ mice ($P > 0.001$) and survived for about the same length of time as $ku80^{-/-}APC^{MIN}$ mice ($P > 0.119$). Thus, Ku80 haploinsufficiency, but not Ku80 deletion, reduced life span in APC^{MIN} mice.

Why did tumor number fail to correlate with life span? It is important to note that tumor number was measured at the end of life. For $Ku80^{+/+}APC^{+/+}$ and $Ku80^{+/-}APC^{+/+}$ mice, ~20 tumors per animal were commonly found at the time of death. This finding suggests that cancer onset and/or progression was more severe in $Ku80^{+/-}APC^{+/+}$ mice compared with $Ku80^{+/+}APC^{+/+}$ mice, but total tumor number was the same. However, the total number of tumors at the end of life was much lower for $ku80^{-/-}APC^{MIN}$ mice. About half of these mice exhibited six or fewer tumors and some exhibited as low as one or two tumors (Fig. 1*A*). Therefore, in addition to tumor burden, the early aging phenotype likely contributed to death in $ku80^{-/-}APC^{MIN}$ mice. Many of the $ku80^{-/-}APC^{+/+}$ mice died from early aging during the life span of the $ku80^{-/-}APC^{MIN}$ mice (Fig. 1*B*), showing that the latter cohort died from a combination of early aging and MIN.

Why does *Ku80* gene dosage fail to correlate with life span? The odd response to *Ku80* gene dosage suggests a balance between two independent events that either increase or reduce the MIN phenotype. We hypothesized that these events are DNA mutations and the DNA damage responses that ultimately lead to deleterious cell fates like cell death or senescence (Fig. 1*C*). We anticipated that $Ku80^{+/+}APC^{MIN}$ mice would harbor a normal level of spontaneous DNA damage that was quickly repaired, resulting in minimal mutations and minimal cell death or senescence. $Ku80^{+/-}APC^{MIN}$ mice might show a small decrease in damage repair that only modestly increases mutations and deleterious cell fates. However, $ku80^{-/-}APC^{MIN}$ mice would be substantially deficient in repairing spontaneous DNA damage, and the accumulated damage would stimulate a significant DNA damage response resulting in cell death or senescence, which would ultimately reduce cancer development. This possibility is supported by the observation that Ku80 haploinsufficiency modestly increases chromosomal breaks (likely due to a small decrease in DNA repair) but does not affect cell proliferation, whereas total Ku80 deletion greatly increases chromosomal breaks and enhances p53-dependent cellular senescence (8, 10, 13). Thus, we hypothesized that complete Ku80 deletion lowers tumor burden by elevating DNA damage responses, and predicted that $ku80^{-/-}$ cells should harbor a greater level of spontaneous DNA damage that induced constitutive cellular damage responses, compared with either $Ku80^{+/+}$ or $Ku80^{+/-}$ cells.

Total Ku80 deletion induces p53-mediated DNA damage responses in fibroblasts and small intestine. Total deficiency in NHEJ was shown to induce cellular senescence (10) and neuronal apoptosis (23), both of which depended on p53 activity. We found p53 to be constitutively activated in $ku80^{-/-}$ MEFs (passage 3) without exposure to DNA-damaging agents. Western blot analyses showed elevated levels of total p53 protein in $ku80^{-/-}$ compared with $Ku80^{+/+}$ and $Ku80^{+/-}$ fibroblasts (Fig. 2*A, top*, compare *lanes 1* and *2* with *lane 3*). In addition, $ku80^{-/-}$ cells showed higher levels of p53 phosphorylated at serine 15 (p53 pS15) than control cells with or without radiation exposure (Fig. 2*A, middle*, compare *lanes 3* and *8* with *lanes 1, 2, 6*, and *7*). p53 serine 15 is phosphorylated by ATM/ATR (ataxia-telangiectasia mutated/ATM and Rad3-related) in response to DNA breaks and is a hallmark of p53 activation (24), supporting the idea shown in Fig. 1*C* that complete Ku80 deficiency, but not Ku80 haploinsufficiency, induced cellular responses to inefficiently repaired DNA breaks.

Next, we measured expression levels of p21, a p53 transcriptional target and a cyclin-dependent kinase inhibitor that can induce cellular senescence (2). Complete Ku80 deficiency increased steady-state p21 levels, detected by Western blotting (Fig. 2*B, top*, compare *lanes 1* and *2* with *lane 3*), in a p53-dependent manner (compare *lanes 3* and *5*). However, Ku80 deficiency did not increase the levels of p16 (Fig. 2*B, middle*, compare *lanes 1* and *2* with *lane 3*), another cyclin-dependent kinase inhibitor that is important for cellular senescence but is not controlled by p53. Quantitative real-time RT-PCR showed that complete Ku80 deficiency increased p21 transcription in small intestine 4 h after exposure to 8-Gy γ-radiation (Fig. 3; compare *blue lanes 4* and *6*; $P = 0.0038$, *t* test) in a p53-dependent manner (Fig. 3, compare *blue lanes 6* and *7*; $P = 0.0091$). By contrast, Ku80 haploinsufficiency did not increase p21 levels (Fig. 3, compare *blue lanes 4* and *5*; $P = 0.8349$). Thus, these observations support our model (Fig. 1*C*) because complete Ku80 deficiency, but not Ku80 haploinsufficiency, enhanced both chronic and acute p53-mediated up-regulation of p21 in MEFs and small intestine. Furthermore, these data support

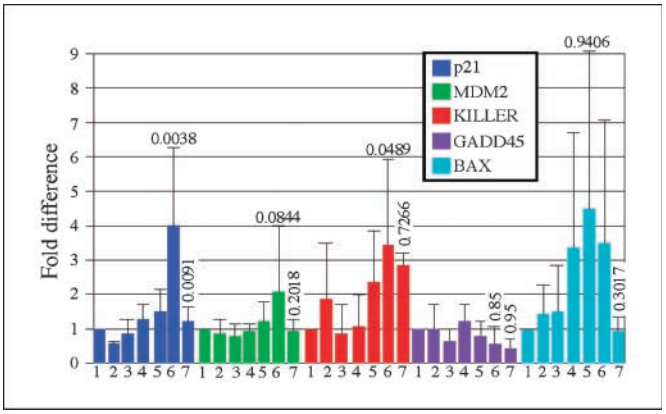

Figure 3. Ku80-mutant small intestines exhibit increased p21 levels that are dependent on p53 in response to 8-Gy γ-radiation as shown by quantitative real-time RT-PCR. *Lanes 1* to *3,* nonirradiated; *lanes 4* to *7,* 8 Gy; *lanes 1* and *4, $ku80^{+/+}$ $p53^{+/+}$. Lanes 2* and *5, $Ku80^{+/-}$ $p53^{+/+}$. Lane 3* and *6, $ku80^{-/-}$ $p53^{+/+}$. Lane 7, $ku80^{-/-}$ $p53^{-/-}$*. The average of three samples is shown for each cohort. Statistics (Student's *t* test) comparing *lanes 4* and *6* are above *lane 6* and statistics comparing *lanes 6* and *7* are above *lane 7*.

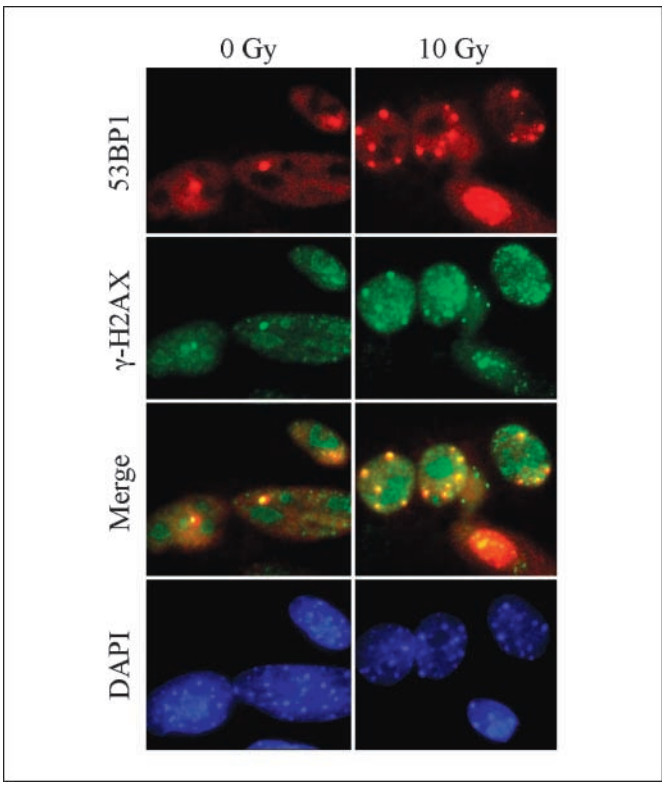

Figure 4. 53BP1 and γ-H2AX colocalize in persistent or spontaneous DNA damage foci in MEFs. MEFs grown on glass slides were mock irradiated or irradiated with 10-Gy X-rays and allowed to recover for 48 h before fixation and staining with the indicated antibodies. *Merge,* the yellow foci show colocalization between 53BP1 (*red*) and γ-H2AX (*green*). *DAPI,* 4′,6-diamidino-2-phenylindole.

our hypothesis that Ku80 deletion inhibits oncogenesis by inducing a p53-mediated DNA damage response.

We also tested levels of other p53-induced transcripts in the small intestine with and without exposure to 8-Gy γ-radiation. These transcripts include MDM2, KILLER/DR5, GADD45, and BAX (3, 24). Quantitative real-time RT-PCR suggests a trend that complete Ku80 deficiency increased MDM2 transcription after exposure to 8-Gy γ-radiation (Fig. 3, compare *green lanes 4* and *6*; $P > 0.0844$) in a p53-dependent manner (Fig. 3, compare *green lanes 6* and *7*; $P > 0.2018$). However, this increase is not as dramatic as the increase in p21 and not significant with the numbers tested. The remaining transcripts do not consistently exhibit a pattern that reflects specificity based on Ku80 dosage (GADD45 and BAX) and/or p53 regulation (KILLER/DR5 and BAX).

Ku80 deficiency increases DNA lesions in fibroblasts and chromosomal rearrangements in small intestine. We next asked whether the elevated p21 levels in *ku80*$^{-/-}$ cells could have resulted from persistent DNA damage. To evaluate DNA lesions, we measured the number of nuclear foci containing 53BP1 in MEFs cultured under physiologic (3%) O_2. We previously showed that *ku80*$^{-/-}$ fibroblasts are hypersensitive to the oxidative stress of atmospheric (21%) O_2 (25). 53BP1 rapidly localizes to DNA double-strand breaks and is a marker of unrepaired DNA damage and an important component of the DNA damage response (26). Accordingly, we find that 53BP1 and γ-H2AX foci colocalize in control MEFs, as well as in persistent DNA damage foci, 48 hours after exposure to 10-Gy X-rays (Fig. 4). Irradiation increased the number of MEF with foci by ~5 fold. Because many γ-H2AX molecules recognize a DNA double-strand break (27) and because 53BP1 and γ-H2AX foci display perfect colocalization, the spontaneous 53BP1 foci observed in nonirradiated MEFs are therefore likely similar to X-ray–induced double-strand breaks. We observed that ~15% of *Ku80*$^{+/+}$ MEFs exhibit one or more 53BP1 foci per nucleus, compared with ~25% of *Ku80*$^{+/-}$ MEFs and ~55% of *ku80*$^{-/-}$ MEFs (Fig. 5*A* and *B*). Thus, Ku80 haploinsufficiency caused a modest but significant increase in 53BP1 foci ($P = 0.0068$, sample *t* test), whereas Ku80 deletion caused a greater increase in 53BP1 foci as compared with both *Ku80*$^{+/+}$ MEFs ($P > 0.0001$) and *Ku80*$^{+/-}$ MEFs ($P > 0.0001$). These findings indicate that most of the *ku80*$^{-/-}$ MEFs harbored persistent unrepaired DNA damage. These data also support our model (Fig. 1*C*) because Ku80 haploinsufficiency increased DNA damage but not p53-mediated DNA damage responses and the levels of DNA lesions were directly dependent on *Ku80* gene dosage.

We also determined the number of gross chromosomal rearrangements in the small intestine of *Ku80*$^{+/+}$ and *ku80*$^{-/-}$ mice that harbor the pUR288-*lacZ* mutation reporter (16). Previously, we showed that the mutations that changed the size of the pUR266-*lacZ* mutation reporter plasmid were gross chromosomal

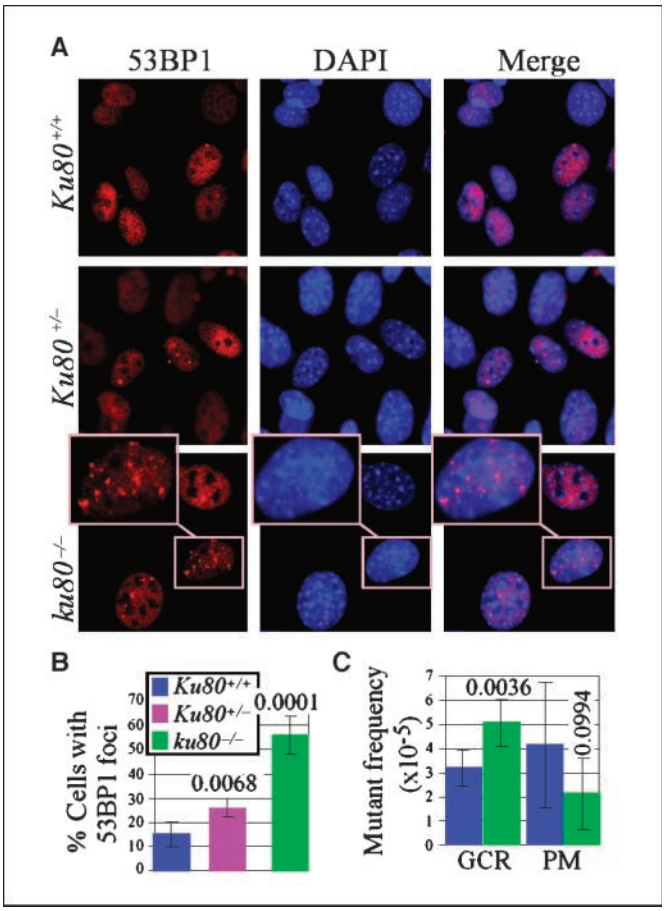

Figure 5. Ku80 deletion increases DNA damage and mutations. *A,* 53BP1 foci in MEFs. Note enlarged inset for one *ku80*$^{-/-}$ nucleus to better visualize 53BP1 foci. *B,* quantitation for 53BP1 nuclear foci after observing 1,239 *Ku80*$^{+/+}$, 838 *Ku80*$^{+/-}$, and 688 *ku80*$^{-/-}$ nuclei. Statistics (Student's *t* test) comparing *Ku80*$^{+/+}$ to *Ku80*$^{+/-}$ nuclei ($P = 0.0068$), *Ku80*$^{+/+}$ to *Ku80*$^{-/-}$ nuclei ($P > 0.0001$), and *Ku80*$^{+/-}$ to *Ku80*$^{-/-}$ nuclei ($P > 0.0001$). *C,* gross chromosomal rearrangements (*GCR*) in small intestine. Statistics comparing gross chromosomal rearrangements in *Ku80*$^{+/+}$ to *ku80*$^{-/-}$ mice ($P > 0.0036$) and point mutations in *ku80*$^{+/+}$ to *ku80*$^{-/-}$ mice ($P > 0.0994$).

rearrangements (large deletions, inversions, or translocations) whereas mutations that did not change the size of the mutation reporter were point mutations or small insertions/deletions (28). Complete Ku80 deletion significantly increased gross chromosomal rearrangements in the small intestine (Fig. 4*C*), supporting the notion that double-strand break repair is chronically defective in the absence of Ku80 function and that an alternative mutagenic pathway repaired these breaks. In addition, we observed a small but not significant decrease in point mutations. Thus, Ku80 deletion impairs double-strand break repair such that some breaks ultimately result in rearrangements; however, these rearrangements do not frequently lead to cancer as long as gatekeeper responses are intact.

Conclusion

DNA repair genes are generally thought to suppress malignant tumorigenesis because they are important for maintaining genomic integrity. Consistent with this view, mutations in some repair genes increase the incidence of cancer in both mice and humans. Ku80 is crucial for the repair of DNA double-strand breaks by the NHEJ pathway and has been described as a tumor suppressor. However, $ku80^{-/-}$ mice, which age rapidly and have a shortened life span, display a very low cancer incidence, suggesting that Ku80 may not act as a tumor suppressor. Nonetheless, it was not clear whether the low cancer incidence was a secondary consequence of the shortened life span or a primary consequence of Ku80 deletion. Here our results show that complete Ku80 deletion reduced the tumor burden of APC^{MIN} mice, which are prone to intestinal tumors but have intact DNA damage responses. Thus, in chronological time, complete Ku80 deletion reduced tumor burden. Our data further suggest that the reduced tumor burden was due to persistent unrepaired DNA double-strand breaks that elevated a p53-dependent DNA damage response. We conclude that Ku80 is not a tumor suppressor but rather enables tumor development, likely by dampening gatekeeper responses (29).

Disclosure of Potential Conflicts of Interest

No potential conflicts of interest were disclosed.

Acknowledgments

Received 6/3/2008; revised 8/20/2008; accepted 9/16/2008.

Grant support: Grants R01 CA76317-05A1 and 3P30 CA054174-16S2 (P. Hasty), NIH UO1 ES11044 (P. Hasty and J. Vijg), P01 AG17242 (P. Hasty, J. Campisi, and J. Vijg), and DOD W81XWH-04-1-0325 (V.B. Holcomb).

The costs of publication of this article were defrayed in part by the payment of page charges. This article must therefore be hereby marked *advertisement* in accordance with 18 U.S.C. Section 1734 solely to indicate this fact.

We thank Charnae Williams for expert technical assistance, Gary Chisholm for statistical analysis (The Department of Epidemiology and Biostatistics, The University of Texas Health Science Center at San Antonio), Dr. Philip Leder (Department of Genetics, Harvard Medical School, Boston, MA) for p21-mutant MEF, Dr. Norman Sharpless (Department of Medicine, Lineberger Comprehensive Cancer Center, University of North Carolina School of Medicine, Chapel Hill, NC) for p16/19-mutant MEFs, and Dr. Larry Donehower for assistance with detecting p53 by Western blot.

References

1. Kinzler KW, Vogelstein B. Gatekeepers and caretakers. Nature 1997;386:761–3.
2. Campisi J, d'Adda di Fagagna F. Cellular senescence: when bad things happen to good cells. Nat Rev Mol Cell Biol 2007;8:729–40.
3. Riley T, Sontag E, Chen P, Levine A. Transcriptional control of human p53-regulated genes. Nat Rev Mol Cell Biol 2008;9:402–12.
4. Lengauer C, Kinzler KW, Vogelstein B. Genetic instabilities in human cancers. Nature 1998;396:643–9.
5. Hoeijmakers JH. Genome maintenance mechanisms for preventing cancer. Nature 2001;411:366–74.
6. Roth DB, Gellert M. New guardians of the genome. Nature 2000;404:823–5.
7. Burma S, Chen BP, Chen DJ. Role of non-homologous end joining (NHEJ) in maintaining genomic integrity. DNA Repair (Amst) 2006;5:1042–8.
8. Karanjawala ZE, Grawunder U, Hsieh CL, Lieber MR. The nonhomologous DNA end joining pathway is important for chromosome stability in primary fibroblasts. Curr Biol 1999;9:1501–4.
9. Li H, Vogel H, Holcomb VB, Gu Y, Hasty P. Deletion of Ku70, Ku80, or both causes early aging without substantially increased cancer. Mol Cell Biol 2007;27:8205–14.
10. Lim DS, Vogel H, Willerford DM, Sands AT, Platt KA, Hasty P. Analysis of ku80-mutant mice and cells with deficient levels of p53. Mol Cell Biol 2000;20:3772–80.
11. Holcomb VB, Vogel H, Marple T, Kornegay RW, Hasty P. Ku80 and p53 suppress medulloblastoma that arise independent of Rag-1-induced DSBs. Oncogene 2006;25:7159–65.
12. Vogel H, Lim DS, Karsenty G, Finegold M, Hasty P. Deletion of Ku86 causes early onset of senescence in mice. Proc Natl Acad Sci U S A 1999;96:10770–5.
13. Holcomb VB, Vogel H, Hasty P. Deletion of Ku80 causes early aging independent of chronic inflammation and Rag-1-induced DSBs. Mech Ageing Dev 2007;128:601–8.
14. Halberg RB, Katzung DS, Hoff PD, et al. Tumorigenesis in the multiple intestinal neoplasia mouse: redundancy of negative regulators and specificity of modifiers. Proc Natl Acad Sci U S A 2000;97:3461–6.
15. Zhu C, Bogue MA, Lim DS, Hasty P, Roth DB. Ku86-deficient mice exhibit severe combined immunodeficiency and defective processing of V(D)J recombination intermediates. Cell 1996;86:379–89.
16. Garcia AM, Busuttil RA, Rodriguez A, et al. Detection and analysis of somatic mutations at a lacZ reporter locus in higher organisms: application to *Mus musculus* and *Drosophila melanogaster*. Methods Mol Biol 2007;371:267–87.
17. Nishisho I, Nakamura Y, Miyoshi Y, et al. Mutations of chromosome 5q21 genes in FAP and colorectal cancer patients. Science 1991;253:665–9.
18. Groden J, Thliveris A, Samowitz W, et al. Identification and characterization of the familial adenomatous polyposis coli gene. Cell 1991;66:589–600.
19. Moser AR, Shoemaker AR, Connelly CS, et al. Homozygosity for the Min allele of Apc results in disruption of mouse development prior to gastrulation. Dev Dyn 1995;203:422–33.
20. Moser AR, Pitot HC, Dove WF. A dominant mutation that predisposes to multiple intestinal neoplasia in the mouse. Science 1990;247:322–4.
21. Su LK, Kinzler KW, Vogelstein B, et al. Multiple intestinal neoplasia caused by a mutation in the murine homolog of the APC gene. Science 1992;256:668–70.
22. Senda T, Iizuka-Kogo A, Onouchi T, Shimomura A. Adenomatous polyposis coli (APC) plays multiple roles in the intestinal and colorectal epithelia. Med Mol Morphol 2007;40:68–81.
23. Gao Y, Ferguson DO, Xie W, et al. Interplay of p53 and DNA-repair protein XRCC4 in tumorigenesis, genomic stability and development [see comments]. Nature 2000;404:897–900.
24. Meek DW. The p53 response to DNA damage. DNA Repair (Amst) 2004;3:1049–56.
25. Parrinello S, Samper E, Krtolica A, Goldstein J, Melov S, Campisi J. Oxygen sensitivity severely limits the replicative lifespan of murine fibroblasts. Nat Cell Biol 2003;5:741–7.
26. Mochan TA, Venere M, DiTullio RA, Jr., Halazonetis TD. 53BP1, an activator of ATM in response to DNA damage. DNA Repair (Amst) 2004;3:945–52.
27. Pilch DR, Sedelnikova OA, Redon C, Celeste A, Nussenzweig A, Bonner WM. Characteristics of γ-H2AX foci at DNA double-strand breaks sites. Biochem Cell Biol 2003;81:123–9.
28. Dolle ME, Giese H, Hopkins CL, Martus HJ, Hausdorff JM, Vijg J. Rapid accumulation of genome rearrangements in liver but not in brain of old mice [see comments]. Nat Genet 1997;17:431–4.
29. Hasty P. Is NHEJ a tumor suppressor or an aging suppressor? Cell Cycle 2008;7:1139–45.

Ku80 Deletion Suppresses Spontaneous Tumors and Induces a p53-Mediated DNA Damage Response

Valerie B. Holcomb, Francis Rodier, YongJun Choi, et al.

Cancer Res 2008;68:9497-9502.